ISSN 1027-4510, Journal of Surface Investigation: X-ray, Synchrotron and Neutron Techniques, 2024, Vol. 18, No. 3, pp. 660–665. © Pleiades Publishing, Ltd., 2024.

Evolution of the Nanohardness of Two-Component Titanium-Based Solutions in the Case of Torsion under High Pressure

Yu. D. Zavorotnev[a], G. C. Davdjan[b], V. N. Varyukhin[a], A. G. Petrenko[a], E. Yu. Tomashevskaya[c], and B. B. Straumal[b, *]

[a] *Galkin Donetsk Institute of Physics and Engineering, Donetsk, 283048 Russia*

[b] *Osipyan Institute of Solid State Physics, Russian Academy of Sciences, Chernogolovka, 142432 Russia*

[c] *Tugan-Baranovsky Donetsk National University of Economics and Trade, Donetsk, 283048 Russia*

**e-mail: straumal@issp.ac.ru*

Received January 12, 2024; revised March 2, 2024; accepted March 2, 2024

Abstract—On the basis of phenomenological theory in the Landau approximation, a model is developed to describe experiments on measuring the nanohardness of two-component titanium-based solutions when torsion is applied under high pressure. The possible mechanisms for the appearance in the experiment of asymmetry of this magnitude relative to the middle of the radius of a cylindrical sample are determined. Additionally, the behavior of the radial and angular components of nanohardness in the presence of a point defect in the material is studied.

Keywords: high-pressure torsion, order parameter, Landau's theory, phase transformations, torque

DOI: 10.1134/S1027451024700277

INTRODUCTION

Currently, titanium alloys are widely used in industry [1–4]. The characteristics of these compounds can be purposefully changed using various alloying elements [5–7]. However, today the need for fundamentally new structural materials is increasing [8–10]. For example, hardened heat-resistant alloys can no longer fully meet the requirements of aerospace technology. Therefore, there is a need to study alloys with other possible additives. In [11], the nanohardness (H) and Young's modulus (E) were measured for three alloys: Ti–2.5 wt % Ni, Ti–2 wt % Cr, and Ti–2.2 wt % Fe, pre-annealed in the two-phase region of the phase diagram (αTi + intermetallic compound) and then subjected to torsion under high pressure. The titanium alloy with the addition of nickel showed the highest values of H and E; they change uniformly from the center to the edge of the sample, and after torsion under high pressure, the alloy contained two phases: α and ω phases. The nanohardness of the alloy Ti–2.5 wt % Ni along the radius of the sample under the surface changes slightly: from a minimum value of 4.8 GPa to a maximum value of 5.2 GPa, as does Young's modulus (from 121 to 155 GPa). The maxima of the H and E values fall in the middle of the sample radius. Ti–2.2 wt % Fe alloy behaves differently: the presence of four phases in it (α, β, ω, and TiFe) leads to a large scatter in the measured values of H and E: from 4.4 to 2.0 GPa and from 131 to 12 GPa, respectively. The processing of P–h diagrams (here P is the load magnitude, h is the indentation depth) made it possible to relate the nanohardness of the material to its creep. However, this study is purely experimental in nature, and, therefore, there is a need for theoretical understanding of the results obtained. In this work, the problem is considered using the phenomenological theory of Landau.

CALCULATION METHOD

Landau's theory showed good results when studying two-component copper-based solutions [12–18] beyond the region of elasticity. Satisfactory agreement with the experiment was obtained by studying the shifts of phase boundaries when applying nondestructive torsion under high pressure, a change in the lattice parameters, and kink propagation. In these works, the dependence of the torsion moment on the number of revolutions is approximated by a hyperbolic tangent. Since the dependence of the observed parameters on the moment is not investigated in this study, the corresponding value will not appear explicitly and will be included in the phenomenological constants. In addition, the potential will not include the Lifshitz invariants, which are responsible for the formation of a spiral structure with a propagation vector along the OZ

axis, since effects arising in the perpendicular *XOY* plane are considered. As stated above, this will be the distribution of the order parameter over the radius and angle in the *XOY* plane, as well as the nanohardness in an ideal crystal and in a crystal with one point defect.

It was noted in [19] that two-component solutions are not actually crystals, since they do not have a lattice structure. However, if we apply the virtual crystal approximation [20], then translational invariance is restored and a generalized vector order parameter can be introduced, which characterizes the change in the linear dimensions and the shape of the unit cell of the virtual lattice under certain influences. In an experiment, this is expressed in a change in the interplanar distance in the crystal lattice and a change in its parameters [21, 22]. Therefore, when considering the task at hand, Landau's phenomenological theory can be applied. Let us write the nonequilibrium thermodynamic potential in the form:

$$\begin{aligned}\Phi_0 &= \gamma_1\left(\left(\frac{\partial q(x,y)}{\partial x}\right)^2+\left(\frac{\partial q(x,y)}{\partial y}\right)^2\right)\\ &+\frac{\alpha_1}{2}q^2(x,y)+\frac{\alpha_2}{4}q^4(x,y)+\frac{\alpha_3}{6}q^6(x,y)\\ &+\sum_{i=1}^{2}\gamma_2\left(x,x+(-1)^i\Delta x,y\right)\\ &\times q^2(x,y)q^2\left(x+(-1)^i\Delta x,y\right)\\ &+\sum_{i=1}^{2}\gamma_2\left(x,y,y+(-1)^i\Delta y\right)\\ &\times q^2(x,y)q^2\left(x,y+(-1)^i\Delta y\right).\end{aligned} \tag{1}$$

where α_i and γ_i ($i = 1, 2, 3$) are the phenomenological parameters, the terms with derivatives describe the inhomogeneities of the structure in the *XOY* plane, the last two sums are responsible for the interaction with nearest neighbors, and $q(x, y)$ is the order parameter.

In the experiment described in [11], the sample is actually acted upon by two torques directed in different directions. These moments lead to different signs of deformation of the edge and center of the sample. As a result, as indicated in [11], in the case of an ideal, impurity-free sample, annihilation occurs at half the radius, and there is no deformation. In fact, there is an anti-symmetric distribution of the order parameter relative to the unperturbed state and the maximum strength of the sample at half the radius. However, the presence of any defect leads to a violation of symmetry and distortion of the distribution of the order parameter along the radius.

Let two opposite moments be instantly applied to the sample. Let us consider the time distribution of the order parameter over the radius and angle. The time dependence of the order parameter during the imposition of torsion under high pressure is described using the Landau–Khalatnikov equation in the form:

$$\frac{\partial q_i}{\partial t} = -\gamma_{ij}\frac{\delta\Phi}{\delta q_j},\quad (i = x, y), \tag{2}$$

where Φ is the free energy functional,

$$\frac{\delta\Phi}{\delta q} = \sum_k (-1)^k \frac{d^k}{dz^k}\frac{\partial\Phi}{\partial\left(\frac{\partial^k q}{\partial z^k}\right)}$$

is the functional derivative, t is time, γ_{ii} ($i = x, y$) is the matrix of kinetic coefficients characterizing the rate of relaxation of the system to the equilibrium position, and q_i are the components of the vector order parameter of the system. In what follows, we will assume that the kinetic coefficients γ_{ii} ($i = x, y$) are constant and, for simplicity, we will neglect cross effects between different components of the order parameter $y_{xy} = y_{yx} = 0$. The order parameter is a linear combination of atomic displacements during phase transition. In experiment, this is expressed in a change in the interplanar distance in the crystal lattice and its parameters [21, 22].

Since a cylindrical sample was used in the experiment, let us consider the problem in a cylindrical coordinate system, after transition to which we obtain:

$$\begin{aligned}\frac{\partial q}{\partial t} &= -\gamma_{ii}\left(-\gamma_1\left(\frac{\partial^2 q(r,\varphi)}{\partial r^2}\right)+\frac{1}{r}\frac{\partial q(r,\varphi)}{\partial r}+\frac{1}{r^2}\frac{\partial^2 q(r,\varphi)}{\partial\varphi^2}\right)\\ &+\alpha_1 q(r,\varphi)+\alpha_2\left(q(r,\varphi)\right)^3+\alpha_3\left(q(r,\varphi)\right)^5\\ &+2\sum_{i=1}^{2}\gamma_2\left(r,r+(-1)^i\Delta r,\varphi\right)\\ &\times q(r,\varphi)q^2\left(r+(-1)^i\Delta r,\varphi\right)\\ &+2\sum_{i=1}^{2}\gamma_2\left(r,\varphi,\varphi+(-1)^i\Delta\varphi\right)\\ &\times q(r,\varphi)q^2\left(r,\varphi,\varphi+(-1)^i\Delta\varphi\right),\end{aligned} \tag{3}$$

where r and φ are polar coordinates characterizing the position of the atom, and Δr and $\Delta\varphi$ are the radial and angular distances to the nearest neighbors.

RESULTS AND DISCUSSION

Let us consider two situations: an ideal crystal and a crystal, in which a point defect is located at some distance from the center. In the first case, in the absence of slipping, the boundary conditions when solving Eq. (3) must be the same in modulus and different in sign. By analogy with the results of [13–15], it can be assumed that there are different values of unit-cell distortion at different annealing temperatures. Also, at a

certain annealing temperature, there should be a steady state, in which there is no deformation of the unit cell; this is confirmed by the results obtained in [3–5]. That is, this state has the greatest nanohardness, and when torsion is applied under high pressure, theoretically no changes occur. It follows from this that all graphs of the dependence of nanohardness on radius should have a common maximum point corresponding to the steady state. The results of calculation are presented in Fig. 1 and qualitatively show the distribution of the order parameter along the radius at different moments of time under the condition that there is a high annealing temperature and, accordingly, low initial distortion. Figure 2 shows the corresponding distribution of nanostrength values *HP* along the radius, which was calculated using the formula:

$$HP = R\frac{a}{a+|q|}, \quad (4)$$

where a is the parameter of the undeformed lattice, q is the deviation of the lattice parameter from the ideal one, which actually coincides with the earlier introduced order parameter, and R is an insignificant parameter for qualitative consideration.

It can be seen that, in accordance with the above reasoning, the distortions in the middle of the radius are equal to zero (Fig. 1). Consequently, the maximum hardness is located here (Fig. 2). However, in the final state, the behavior of the *HP* graph differs from the experimental data (Fig. 2, [11]). Apparently, this discrepancy is caused by a small number of measurements. As is known from statistics, for the reliable interpretation of any curve it is necessary to have three more measurement points than curve parameters. In particular, a straight line has two parameters. Therefore, in order for the sampling of experimental measurements to be representative for the reliable interpretation of a linear relationship, it is necessary to have a minimum of five experimental points. Any curve has a larger number of parameters and, therefore, a larger sampling size is necessary. In [11], the curve of strength in Fig. 2 is based on three points, which is clearly not enough for reliable interpretation of the *HP* behavior. Another possible reason could be the approach of the nearest neighbors. In a real crystal, a large number of atoms participate in the interaction. One cannot exclude the possibility that the theory is incomplete and does not take into account some important mechanisms that influence the behavior of the order parameter during torsion.

It is of interest to study the behavior of the order parameter and *HP* under conditions of sample slipping, which can occur both at the center and at the edges. In this case, a steady state may not be achieved.

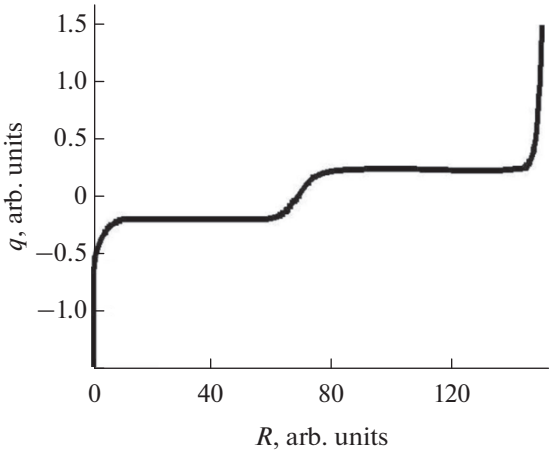

Fig. 1. Time-finite distribution of the order parameter along the radius.

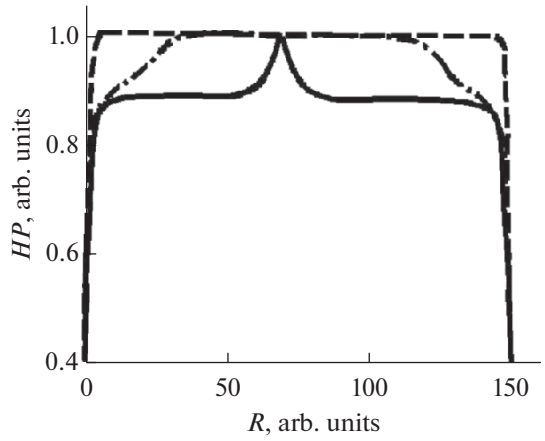

Fig. 2. Distribution of sample hardness along the radius: dashed, dash-dotted, and solid lines indicate the initial moment of time, intermediate time value, and final state, respectively.

Two types of slipping should be distinguished: strong, in which deformations at the center and the edges are of the same sign and different in modulus; and weak, in which the deformations at the center and the edges are different in sign and modulus. Figures 3 and 4 show graphs of the *HP* time dependence in the case of strong and weak slipping. In the case of strong slipping, there is no central peak in the graph of the hardness dependence (Fig. 3) and the curve qualitatively coincides with the corresponding dependence for Ti–2.2 wt % Fe (Fig. 2, [11]).

Figure 5 shows the *HP* dependence in the case when the values of the order parameter at the center and at the edge are approximately equal to the steady-state one and less, but different in modulus. It can be seen that there is no maximum within the range of

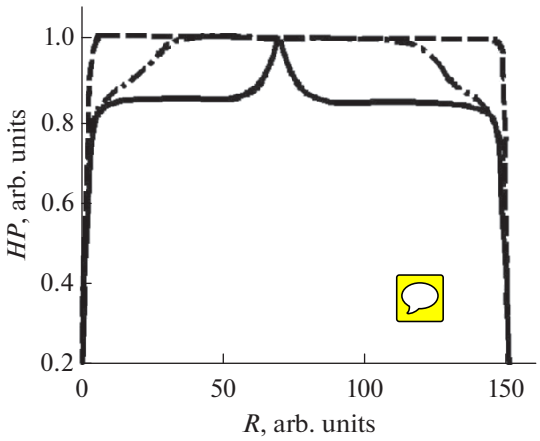

Fig. 3. Distribution of the sample hardness along the radius in the case of strong slipping: dashed, dash-dotted, and solid lines indicate the initial time, intermediate time value, and final state, respectively.

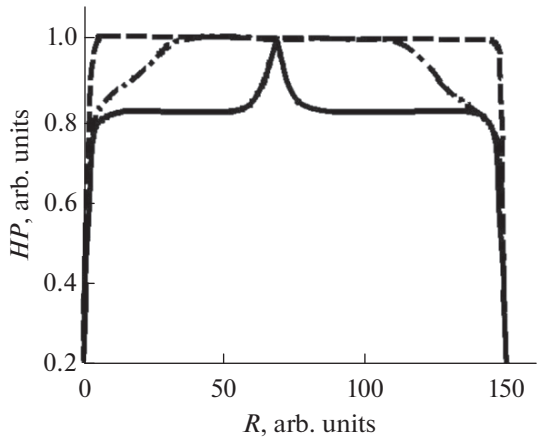

Fig. 4. Distribution of the sample hardness along the radius in the case of weak slipping: dashed, dash-dotted, and solid lines indicate the initial time, intermediate time value, and final state, respectively.

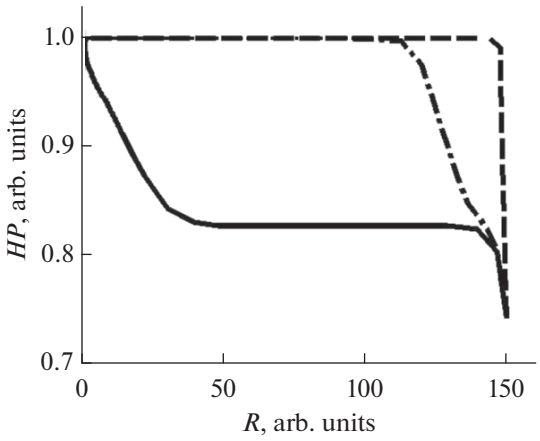

Fig. 5. Distribution of the sample hardness along the radius in the case of strong slipping: dashed, dash-dotted, and solid lines indicate the initial time, intermediate time value, and final state, respectively. The order parameter at the center is less than the steady-state one.

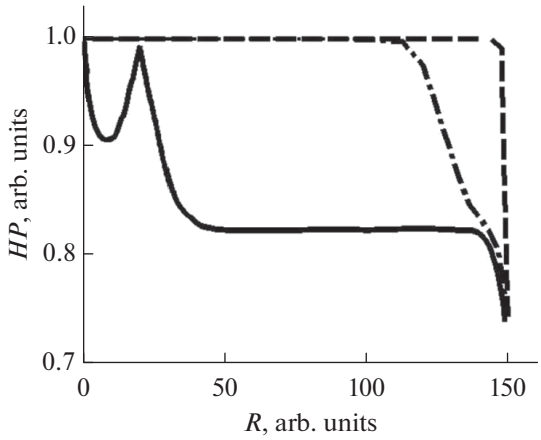

Fig. 6. Distribution of the sample hardness along the radius in the case of weak slipping: dashed, dash-dotted, and solid lines indicate the initial time, intermediate time value, and final state, respectively. The values of the order parameter at the center and at the edges are of different signs with respect to the steady-state one.

radius values, and the curve qualitatively corresponds to the experimental curve for Ti–2 wt % Cr (Fig. 2, [11]). If the order parameter at the center is approximately equal to the steady-state one and greater than its value at the edge, a local maximum appears (Fig. 6), which indicates that the steady state is achievable.

Let us assume that at a certain value of the radius not equal to the middle and at a certain angle, there is a point defect, which is characterized by a certain value of the order parameter. Figure 7 shows the time evolution of the radial distribution of the order parameter in the direction of the defect. It is obvious that the anomaly introduces a significant disturbance into the distribution. At the point, where the defect is located, a local minimum in the nanostrength is observed. There is also a local maximum, which indicates the intersection of the steady state. Of interest is the distribution of nanostrength over an angle in the vicinity of the point, where the defect is located. Figure 8 shows the dependence of the order parameter on the angle, and Fig. 9 shows the corresponding dependence of the nanostrength. It can be seen that these dependences are oscillatory in nature. Due to the fact that the curve of the order parameter turns to zero four times, there are four symmetrical points of maximum nanohardness (Fig. 9).

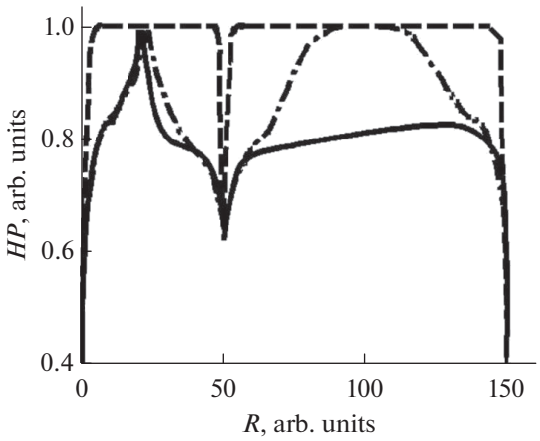

Fig. 7. Distribution of the sample nanostrength along the radius in the direction of the defect: dashed, dash-dotted, and solid lines indicate the initial moment of time, intermediate time value, and final state, respectively.

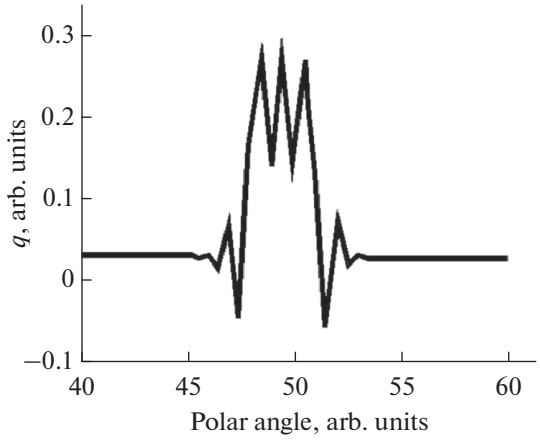

Fig. 8. Distribution of the order parameter over the angle in the vicinity of the defect location point.

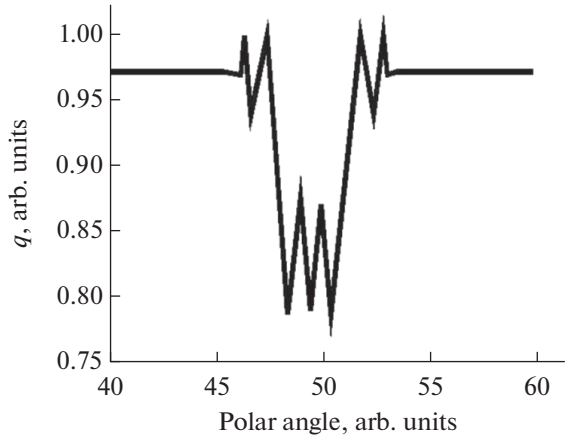

Fig. 9. Distribution of the nanostrength by angle in the vicinity of the point where the defect is located.

CONCLUSIONS

On the basis of phenomenological theory in the Landau approximation, it is shown that in an ideal compound, the maximum nanohardness under high pressure torsion is in the middle of the radius of a cylindrical sample.

The assumption of the possibility of sample slipping at the edges and in the center allowed explanation of the asymmetry of the nanohardness values relative to the middle of the radius and the shift of the maximum nanohardness.

The presence of a point defect in the sample leads to significant distortion of the dependence of the radial and angular components of nanohardness. At the location of the defect, there is a local minimum of nanohardness, and in the immediate vicinity, the radial and angular components acquire an oscillating character.

FUNDING

The study was carried out with financial support of the Ministry of Science and Higher Education of the Russian Federation (agreement 075-15-2023-609, grant no. 13.2251.21.0224).

CONFLICT OF INTEREST

The authors of this work declare that they have no conflict of interest.

REFERENCES

1. D. Özyürek and S. Tekeli, High Temp. Mater. Processes **30**, 175 (2011). https://doi.org./0.1515/HTMP.2011.026
2. M. Wang, X. Lin, and W. Huang, Mater. Technol. **31**, 90 (2016). https://doi.org./10.1179/1753555715Y.0000000079
3. C. Cui, B. M. Hu, L. Zhao, and S. Liu, Mater. Des. **32**, 1684 (2011). https://doi.org./10.1016/j.matdes.2010.09.011
4. A. Pramanik and A. K. Basak, Metals **13**, 1536 (2023). https://doi.org./10.3390/met13091536
5. Z. Zhao, H. Ji, Y. Zhong, C. Han, and X. Tang, Materials **15**, 8589 (2022). https://doi.org./10.3390/ma15238589
6. X. D. Hong, H. R. Zheng, and D. Liang, Mater. Lett. **304**, 130717 (2021). https://doi.org./10.1016/j.matlet.2021.130717
7. M. Thomas and M. Jackson, Scr. Mater. **66**, 1065 (2012). https://doi.org./10.1016/j.scriptamat.2012.02.049
8. L. Bolzoni, E. Herraiz, E. M. Ruiz-Navas, and E. Gordo, Mater. Des. **60**, 628 (2014). https://doi.org./10.1016/j.matdes.2014.04.019

9. G. Markovic, V. Manojlovic, J. Ruzic, and M. Sokic, Materials **16**, 6355 (2023). https://doi.org./10.3390/ma16196355
10. J. Dai, J. Zhu, C. Chen, and F. Weng, J. Alloys Compd. **685**, 784 (2016). https://doi.org./10.1016/j.jallcom.2016.06.212
11. A. S. Gornakova, B. B. Straumal, Yu. I. Golovin, N. S. Afonikova, T. S. Pirozhkova, and A. I. Tyurin, J. Surf. Invest.: X-Ray, Synchrotron Neutron Tech. **15**, 1154 (2021). https://doi.org/10.31857/S102809602111008X
12. Yu. D. Zavorotnev, L. S. Metlov, A. M. Glezer, A. Yu. Zakharov, and E. Yu. Tomashevskaya, J. Phys.: Conf. Ser. **1658**, 012080 (2020). https://doi.org./10.1088/1742-6596/1658/1/012080
13. A. Korneva, A. Kilmametov, Yu. Zavorotnev, L. Metlov, O. Popova, and B. Baretzky, Mater. Lett. **302**, 130386 (2021). https://doi.org./10.1016/j.matlet.2021.130386
14. B. B. Straumal, A. R. Kilmametov, A. Korneva, P. Zieba, Y. Zavorotnev, L. Metlov, O. Popova, and B. Baretzky, Crystals **11**, 766 (2021). https://doi.org./10.3390/cryst11070766
15. Yu.D. Zavorotnev, P.B. Straumal, E.Yu. Tomashevskaya, and B.B. Straumal, Poverkhn.: Rentgenovskie, Sinkhrotronnye Neitr. Issled. 18 (4), 2024.
16. P. Straumal, Y. Zavorotnev, L. Metlov, and O. Popova, Materials **15**, 6970 (2022). https://doi.org./10.3390/ma15196970
17. B. B. Straumal, Yu. D. Zavorotnev, L. S. Metlov, P. B. Straumal, A. G. Petrenko, and E. Yu. Tomashevskaya, Phys. Met. Metallogr. **123**, 1208 (2023). https://doi.org/10.1134/S0031918X22601111
18. Yu. D. Zavorotnev, L. S. Metlov, and E. Yu. Tomashevskaya, Fiz. Tverd Tela **64**, 462 (2022). https://doi.org./10.21883/FTT.2022.04.52186.263
19. A. V. Shubnikov, Zap. Vses. Mineral. O-va. **85**, 108 (1956).
20. G. Erenreikh and L. Shvarts, *Electronic Structure of Alloys* (Mir, Moscow, 1979) [in Russian].
21. SB. B. Straumal, A. R. Kilmametov, Y. Ivanisenko, L. Kurmanaeva, B. Baretzky, Y. O. Kucheev, P. Zieba, A. Korneva, and D. A. Molodov, Mater. Lett. **118**, 111 (2014). https://doi.org./10.1016/j.matlet.2013.12.042
22. B. B. Straumal, A. R. Kilmametov, B. Baretzky, O. A. Kogtenkova, P. B. Straumal, L. Litynska-Dobrzynska, R. Chulist, A. Korneva, and P. Zieba, Acta Mater. **195**, 184 (2020). https://doi.org./10.1016/j.actamat.2020.05.055

Translated by S. Rostovtseva

SPELL: 1. OK